

Protein-Engineered Injectable Hydrogel to Improve Retention of Transplanted Adipose-Derived Stem Cells

Andreina Parisi-Amon, Widya Mulyasmita, Cindy Chung, and Sarah C. Heilshorn*

Stem cell transplantation is a potential therapeutic strategy for multiple injuries and degenerative diseases. Direct stem cell injection at the target site is the clinically preferred method of transplantation due to its minimal invasiveness. Unfortunately, current methods of delivery typically result in low cell survival and retention.^[1–4] Transplanted cell survival is critical to therapeutic success, as functional recovery correlates with the number of viable donor cells.^[3,5] Pre-encapsulation of stem cells within a hydrogel can improve viability by providing bio-mechanical protection,^[6] biochemical survival cues,^[3] and scaffolding.^[7–9] Thixotropic hydrogels that shear-thin under load and quickly recover upon load removal are particularly well suited as injectable cell carriers.^[10–12] Rapid self-healing localizes cells to the targeted area, increasing the probability of post-injection cell retention and engraftment.^[12]

Biopolymer hydrogels commonly used in injection studies include alginate, collagen, and Matrigel.^[3,8,13,14] While commercially available, these naturally derived materials face several shortcomings limiting their efficacy. First, their biochemical and mechanical properties are subject to batch-to-batch variations, leading to inconsistent performance. Second, their sol-gel transitions require dramatic changes in solution parameters (e.g., ionic strength for alginate, pH for collagen, and temperature for Matrigel), exposing cells to non-physiological conditions during encapsulation. Furthermore, Matrigel, while performing well in pre-clinical cell injection studies,^[3,8] is derived from murine sarcoma, making it unsuitable for clinical use due to immunogenic and pathogenic concerns.^[15] These inadequacies have motivated the design of novel self-assembling materials that mimic the natural extracellular matrix.^[16]

Towards this goal, we recently reported the development of recombinant protein polymers that form mixing-induced two-component hydrogels (MITCH).^[17] Fundamental polymer physics and protein thermodynamics were used to directly

control the rheological properties of MITCH through molecular level design.^[18] Briefly, MITCH is composed of two block copolymers, C7 and P9, that contain seven and nine repeats of the CC43 WW domain (C) and the proline-rich peptide (P), respectively (Figure 1a). The C and P peptides bind through specific interactions with a 1:1 stoichiometry.^[19] To impart chain flexibility and solubility, the binding domains are connected by hydrophilic spacers, which also include the tripeptide RGD cell-binding domain in C7. Harnessing recombinant DNA technology, these modular constructs are expressed with high fidelity in *Escherichia coli*, producing polymers with exact molecular sizes, as verified through gel electrophoresis and Western blotting (Figure 1b). Upon mixing the C7 and P9 protein solutions, the two liquid components assemble into a compliant gel (Figure 1c). Network assembly is driven spontaneously by specific recognition between the hetero-assembling peptides, allowing consistent gel formation and cell encapsulation through simple mixing at constant physiological conditions, irrespective of culture media composition.^[17]

In addition to the simple and cyto-compatible encapsulation protocol, MITCH exhibits shear-thinning and self-healing thixotropic properties.^[17] MITCH's transient, non-covalent crosslinks allow network disassembly under reasonable shear forces, making the gel hand-injectable through a 28-gauge needle. After force removal, the transient crosslinks reform to restore the gel network (Figure 1c). These results suggest that MITCH may be an ideal cell delivery vehicle capable of (i) encapsulating cells at constant physiological conditions, (ii) shear-thinning to deliver cells at an injection site using only hand force, (iii) self-healing to re-encapsulate and localize cells at the targeted injection site, and (iv) providing a cyto-compatible scaffold for cell adhesion.

In this study, we report that MITCH promotes the post-injection survival of adipose-derived stem cells (ASCs) in a pre-clinical mouse model. ASCs hold tremendous potential in eradicating many bottlenecks impeding stem cell therapies.^[20,21] ASCs circumvent ethical and procurement challenges because they are harvested in significant numbers through voluntary lipoaspiration of adult fat tissue. The possibility of autologous transplantation also greatly reduces immune rejection concerns. Furthermore, these multipotent cells can differentiate along any of the mesenchymal lineages and are readily reprogrammed into induced pluripotent stem cells.^[22] To demonstrate the cyto-compatibility of MITCH with this clinically important cell type, harvested primary human ASCs (hASCs) were mixed with C7 and P9 solutions to form 3D hydrogel cultures with cells encapsulated throughout. After 10 days of *in vitro* culture, LIVE/DEAD staining revealed maintenance of a uniform distribution of highly viable (>90%) hASCs (Figure 2a). Visualization of polymerized F-actin showed mature and well-spread

A. Parisi-Amon, W. Mulyasmita
Bioengineering, Stanford University
Stanford, CA 94305, USA

Dr. C. Chung
Materials Science and Engineering
& Mechanical Engineering,
Stanford University
Stanford, CA 94305, USA

Prof. S. C. Heilshorn
Materials Science and Engineering
476 Lomita Mall, McCullough 246,
Stanford University
Stanford, CA 94305, USA
E-mail: heilshorn@stanford.edu



DOI: 10.1002/adhm.201200293

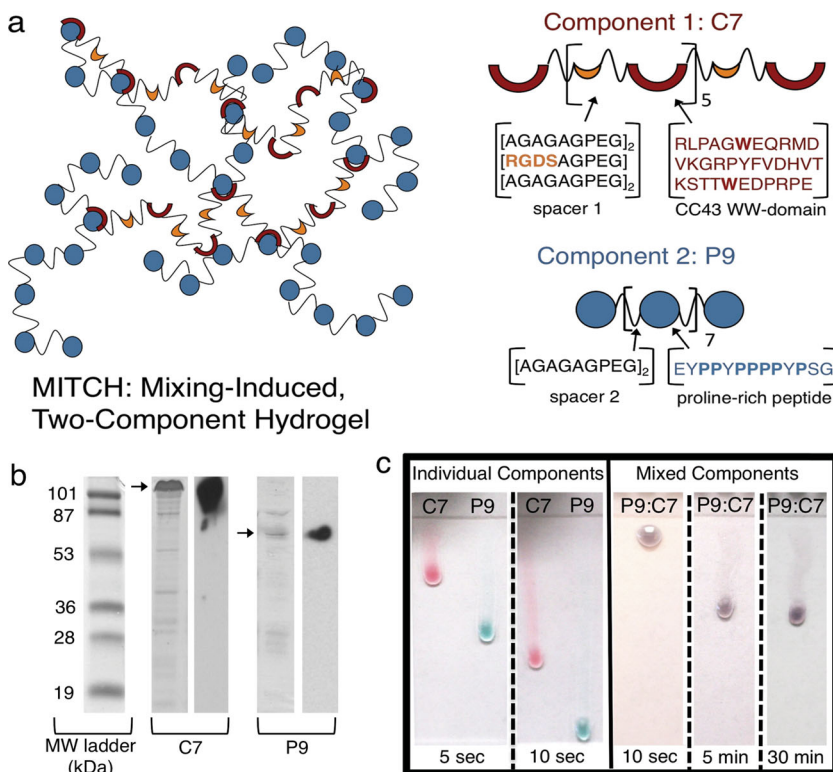


Figure 1. (a) Schematic of MITCH. Hydrogel network (left) formed after mixing of individual components (right). Respective protein sequences shown using single letter amino acid abbreviations. (b) Sodium dodecyl sulfate polyacrylamide gel electrophoresis (SDS-PAGE) (left) and Western blots (right) of purified proteins. Bands of interest indicated by arrows. (c) Ejection of individual (left) or pre-mixed (right) components onto vertical glass slides demonstrating the sol-gel phase transition upon simple mixing of the individual liquid components. Food coloring was added for enhanced visualization: C7 in red and P9 in blue, resulting in a purple P9:C7 mixture. Individual components flow as liquids, covering the length of the slide within 10 s; mixed components solidify into a gel and resist flow for 30 min.

cytoskeletal morphology, implying stable cell-matrix interactions, as expected for cells grown in a matrix presenting RGD cell-binding domains (Figure 2b).^[23]

Successful translation of ASC injection therapy to human clinical trials requires characterization through *in vivo* animal models. The cell-protective and retentive properties of MITCH in an *in vivo* milieu were evaluated by injecting encapsulated mouse ASCs subcutaneously into mice and monitoring post-injection cell viability over time using *in vivo* bioluminescence imaging (BLI). BLI, an emerging molecular imaging technology, relies on the detection of visible light emitted from luminescent cells.^[24,25] Contrary to end-point, histology-based analysis, *in vivo* BLI affords minimally invasive, real-time, and spatiotemporally resolved detection of metabolically active cells in the same living subjects over the course of an experiment.^[13] To enable this imaging modality, we harvested primary ASCs from transgenic mice constitutively expressing firefly luciferase (mASCs^{Fluc+}), which in the presence of oxygen and ATP catalyzes the conversion

of D-luciferin into oxyluciferin. The long-wavelength visible light (>600 nm) emitted during this conversion can penetrate several centimeters of tissue and can thus be captured outside the body with a high-sensitivity charge-coupled device camera.^[24] Similar to the results with primary human ASCs, the mASCs^{Fluc+} retained high viability upon encapsulation in MITCH and exhibited robust cytoskeletal morphology in 3D *in vitro* cultures (Figure 2c).

To study transplantation ability, mASCs^{Fluc+} were injected subcutaneously into the dorsa of athymic nude mice immediately following encapsulation in MITCH. The cell-gel constructs yielded readily under hand injection force and recovered as compact gel structures, visibly observed as palpable nodules at the injection sites (Figure 3a, left). For direct comparison with other clinically relevant materials, mASCs^{Fluc+} were also encapsulated in collagen and alginate, which are commonly used as cell delivery vehicles in pre-clinical studies and are FDA-approved for other medical applications. As with all polymeric hydrogels, the pore size, mechanical properties, and polymer concentration are interrelated for collagen, alginate, and MITCH materials. Because these three biopolymers form gels through different crosslinking mechanisms, it is impossible to match all three parameters across all three hydrogels. Therefore, we chose to synthesize hydrogel formulations with similar storage moduli for comparison in this experiment. We selected an alginate hydrogel formulation that was previously found to provide significant cell protection during syringe needle flow,^[6] thereby setting a high standard for comparison. The formulations of the other two injectable materials (collagen and MITCH) were specifically tailored to have similar plateau storage moduli as the alginate sample ($G' \sim 30$ Pa) (Figure S1 of the Supporting Information (SI)). Cell delivery within saline was included as a negative control. To minimize location-specific bias, injection sites were randomized and rotated across

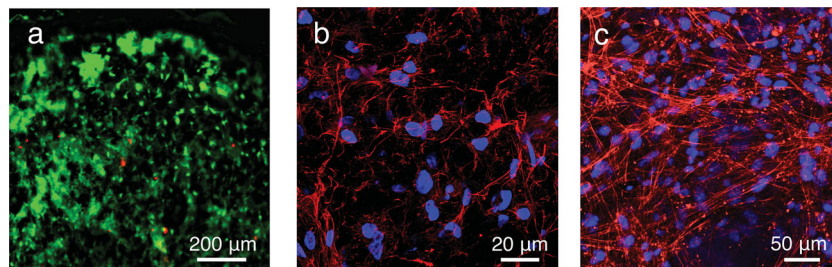


Figure 2. *In vitro* ASC 3D culture in MITCH. (a) hASCs viability after 10 days (live, calcein AM (green); dead, ethidium homodimer (red)). (b) Well-spread hASCs after 10 days (nuclei, DAPI (blue); F-actin, phalloidin (red)). (c) Well-spread mASCs^{Fluc+} after 3 days (nuclei, DAPI (blue); F-actin, phalloidin (red)).

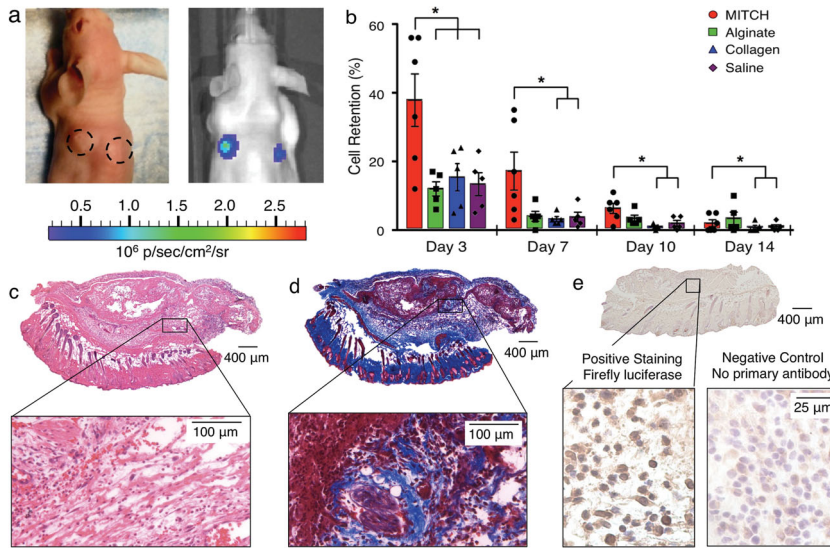


Figure 3. mASCs^{Fluc+} transplantation into nude mice. (a) Representative mouse with injection sites demarcated with dotted lines (day 0, left) and with BLI total flux overlay (day 3, right). (b) BLI measurements of cell retention. Data normalized to day 1 and reported as mean \pm SEM; $n = 5$ or 6 ; $*p < 0.0001$. (c) Hematoxylin and eosin staining of day 3 MITCH-ASC explant (cell nuclei, blue; red blood cells, red; protein and cytoplasm, pink). (d) Trichrome staining of day 3 MITCH-ASC explant (cell nuclei, black; muscle and erythrocytes, red; fibrin, pink; collagen, blue). (e) Immunohistochemical staining of injected mASCs^{Fluc+} in day 3 MITCH-ASC explant. Positive staining with firefly luciferase antibody (positive cells, brown, left) and negative control staining with no primary antibody (right). All cell nuclei counterstained with hematoxylin (blue).

experimental subjects. MITCH samples without cells were also transplanted in the same manner.

The presence of metabolically active mASCs^{Fluc+} was tracked and quantified for 14 days post-injection using BLI following intraperitoneal delivery of D-luciferin. No signal was emitted from off-target sites, suggesting localization of the bulk cell grafts to their original sites of injection (Figure 3a, right). While viable cells were present in all samples throughout the 14-day observation window, mASCs^{Fluc+} encapsulated in MITCH exhibited the highest percentages of retention throughout day 10 (Figure 3b). At day 3, cell retention in MITCH was more than 3-fold greater than in alginate and more than 2-fold greater than in collagen or saline, yielding a statistically significant improvement ($p < 0.0001$). Compared with collagen, the greatest improvement was observed at day 10, when MITCH yielded a more than 7-fold increase in retained, viable cells ($p < 0.0001$). Over the 14-day time course, a decline in BLI readouts and diminishing visual appearance of transplant nodules was observed across all samples, presumably due to biomaterial degradation and cell migration and/or death outpacing cell proliferation. Nevertheless, at day 14, cell retention in MITCH was still significantly enhanced compared to that in collagen or saline, with a greater than 2-fold improvement ($p < 0.0001$). Although the transplanted cell signal was substantially diminished at day 14, previous studies have reported that even short-term viability of transplanted cells can be sufficient to initiate endogenous remodeling. For example, vascular scaffolds with transplanted cells were more efficacious than cell-free scaffolds, despite the death of almost all transplanted cells by day 1 post implantation.^[26] Therefore, the ability to significantly improve

initial ASC retention at the injection site could be valuable in enhancing the efficacy of potential stem cell transplantation therapies.

Explants were obtained from the injection sites at days 3 and 14. Luciferase immunohistochemical staining of day 3 explants qualitatively corroborated the BLI data, showing the presence of transplanted, luciferase-positive cells in all samples (Figure 3e, Figure S2 of the SI). As expected, hematoxylin and eosin staining of day 3 explants revealed the infiltration of host lymphocytes, macrophages, and small vasculature in all samples (Figure 3c, Figure S3 of the SI). In blinded histological analysis, all samples were scored as having mild acute inflammation consistent with injection injury and not exacerbated by material presence. At day 14, nodules were no longer externally visible, however implants were located and harvested upon internal examination of the skin via post-mortem gross dissection. Qualitatively, saline samples had the most compliant and loosely attached nodules, while collagen samples were very dense and compact, which prevented accurate histological sectioning. By comparison, alginate and MITCH samples had intermediate consistencies. Blinded histological analysis reported no evidence of remnant biomaterial in the MITCH and alginate day-14 samples

and no visible sign of sarcoma formation. The role of MITCH in furnishing a temporary and biodegradable scaffold as cells secrete and remodel their native extracellular matrix is a desirable property, as it reduces the risk of chronic foreign-body reactions and eliminates subsequent implant removal surgeries.

Trichrome staining of day 3 and day 14 explants revealed the presence of extracellular matrix deposition within all injection sites with transplanted cells, suggesting possible matrix remodeling by delivered mASCs^{Fluc+} or endogenous cells (Figure 3d, Figure S4 of the SI). To further confirm the role of transplanted ASCs, cell-free MITCH constructs were also injected following the same protocol. Unlike cell-encapsulating constructs, all externally palpable nodules and visible traces of the cell-free constructs by gross dissection were gone by day 3, indicating complete material degradation and an absence of significant extracellular matrix remodeling when no cells are delivered. This suggests a synergy in delivering cells with MITCH, where the presence of MITCH allows for increased cell retention, in turn instigating an increase in matrix deposition within the host. Consistent with this observation, many pre-clinical and clinical studies utilizing ASCs suggest that a key role in functional recovery is through the secretion of paracrine factors.^[4,27,28] These ASC-secreted factors modulate the behavior of endogenous cells to promote regeneration; therefore, direct functional integration of the ASCs into host tissue is not required. Increasing cell retention at the injury site through MITCH-encapsulated delivery is expected to decrease the number of implanted cells needed to achieve equivalent levels of secreted paracrine factors and to promote the regenerative activity of endogenous cells.

We hypothesize that the significant enhancement in cell retention displayed by MITCH may be ascribed to one or more of three distinct phases of cell-material interactions that have been designed into the hydrogel. First, this hydrogel has been designed to enable gentle cell encapsulation, achieved through simple mixing at constant physiological conditions. This allows for the cells to be maintained at optimal physiological conditions prior to syringe needle shearing and transplantation. In contrast, encapsulation within either collagen or alginate requires the cells to be exposed transiently to non-physiological conditions of low pH and high calcium concentration, respectively. Second, the MITCH material, similar to alginate hydrogels, forms the gel phase within seconds after combining the individual components. Therefore, the cells are encapsulated within a fully formed hydrogel inside the syringe before injection takes place. The presence of a gel phase surrounding the cells has been shown to provide mechanical protection to cells encapsulated within alginate during syringe needle flow,⁶ and may also lead to protection of cells in MITCH by a similar mechanism. In contrast, the significant time lag of ~30 minutes required for complete gelation of collagen makes it unable to provide this mechanical cell protection during injection, presumably leading to a decrease in cell viability. Third, MITCH presents the RGD integrin-binding ligand, which is known to elicit favorable cell-matrix adhesion interactions that promote cell viability, with 10 wt% MITCH containing ~ 5.06 mM RGD ligands. While native collagen type I is naturally cell adhesive and includes several cell adhesion ligands, it is a harvested material. Therefore, the level and composition of cell adhesion ligands are unspecified and potentially variable depending on isolation protocol and source. In contrast, alginate does not include any cell-specific ligands to promote cell adhesion. Taken together, MITCH has been designed to provide cell protection during all three stages of cell transplantation within a single material formulation: a gentle cell encapsulation process, mechanical protection during syringe needle flow, and integrin-specific biochemical signaling to support cell adhesion.

Based on these results, MITCH is a promising cell transplantation scaffold that significantly improves the retention of transplanted cells and could be valuable in the development of stem cell injection therapies. In its current formulation, MITCH achieves significant enhanced retention of clinically relevant ASCs at a subcutaneous injection site up to two weeks post-implantation, a time period that may be sufficient to promote endogenous regeneration. Viability of transplanted cells could be further improved by the encapsulation of various pro-survival cocktails in MITCH together with donor cells. Due to the specific peptide-peptide binding interactions that drive assembly at constant physiological conditions and without chemical reaction, bioactive factors can be easily encapsulated within MITCH without affecting hydrogel mechanics¹⁷ or exposing the factors to denaturing conditions. Additionally, taking advantage of modular recombinant protein engineering, future design iterations can be implemented at the amino-acid level, such as encoding pro-survival peptide sequences directly into the polymer backbone. Given the versatility of MITCH, it is an ideal platform upon which to build even more sophisticated scaffolds to target a myriad of specific applications. Future studies include translating this work from proof-of-concept subcutaneous studies into murine models of injury and disease

to characterize the potential benefits of MITCH-delivered ASCs for mesenchymal tissue regeneration.

Experimental Section

Recombinant synthesis of engineered proteins: C7 and P9 were cloned, synthesized, and purified as previously reported and detailed in the SI.¹⁷

ASC harvest: Experiments followed protocols approved by the Stanford Administrative Panel on Laboratory Animal Care. NIH guidelines for the care and use of laboratory animals (NIH Publication #85-23 Rev. 1985) were observed. Mouse ASCs were harvested and processed from inguinal fat pads from five-week-old GFP/firefly luciferase double transgenic mice (Jackson Laboratory) as detailed in the SI. Human ASCs were harvested from human lipoaspirate from the flank and thigh regions by suction assisted liposuction and processed as detailed in the SI. All tissue donors responded to an Informed Consent approved by the Stanford Institutional Review Board.

In vitro cell encapsulation: ASCs were first mixed with P9 solution and then C7 and cultured in a polydimethylsiloxane mold bonded to a glass coverslip (final density 100 000 cells/ml). Cell viability was assessed with LIVE/DEAD staining. Cell nuclei and F-actin were visualized through staining with 6-diamidino-2-phenylindole (DAPI) and rhodamine-conjugated phalloidin, respectively. Details provided in the SI.

Cell transplantation: Experiments followed protocols approved by the Stanford Administrative Panel on Laboratory Animal Care. NIH guidelines for the care and use of laboratory animals (NIH Publication #85-23 Rev. 1985) were observed. mASCs^{Fluc+} were encapsulated in either MITCH, alginate (molecular weight = 75 kDa; NovaMatrix), rat tail type I collagen (BD Biosciences), or saline and injected subcutaneously through a 28-gauge, 1-mL insulin syringe into the dorsum of athymic nude mice (25–30 g, male, Charles River Laboratories) anesthetized with isoflurane. Each sample (50 μ L) contained 1×10^6 cells. BLI was performed with an IVIS imaging system (Xenogen Corp.), and data was acquired with LivingImage software (Xenogen Corp.) on days 1, 3, 7, 10, and 14. At days 3 and 14 post-injection, samples were explanted from euthanized mice and processed for blinded histological analysis. Details provided in the SI.

Supporting Information

Supporting Information is available from the Wiley Online Library or from the author.

Acknowledgements

The authors acknowledge funding from CIRM RT2-01938, NIH DP2-OD-006477, and Stanford Bio-X IIP4-22; National Science Foundation Graduate Fellowship (A.P.-A.); Stanford Graduate Fellowship (W.M.); and American Heart Association Fellowship (C.C.). The authors thank Michael Longaker, Allison Nauta, and Benjamin Levi (Stanford Medical School) for assistance with ASC harvesting; Daniel Montoro, Richard Luong, and Pauline Chu (Stanford Cell Imaging and Histology Center) for assistance with histology; and Tim Doyle (Stanford Molecular Imaging Program) for assistance with BLI.

Received: August 20, 2012

Published online:

- [1] M. Zhang, D. Methot, V. Poppa, Y. Fujio, K. Walsh, C. E. Murry, *J. Mol. Cell. Cardiol.* **2001**, *33*, 907.
- [2] T. M. Bliss, S. Kelly, A. K. Shah, W. C. Foo, P. Kohli, C. Stokes, G. H. Sun, M. Ma, J. Masel, S. R. Kleppner, T. Schallert, T. Palmer, G. K. Steinberg, *J. Neurosci. Res.* **2006**, *83*, 1004.

- [3] M. A. Laflamme, K. Y. Chen, A. V. Naumova, V. Muskheli, J. A. Fugate, S. K. Dupras, H. Reinecke, C. Xu, M. Hassanipour, S. Police, C. O'Sullivan, L. Collins, Y. Chen, E. Minami, E. A. Gill, S. Ueno, C. Yuan, J. Gold, C. E. Murry, *Nat. Biotechnol.* **2007**, *25*, 1015.
- [4] M. Tobita, H. Orbay, H. Mizuno, *Discov. Med.* **2011**, *11*, 160.
- [5] G. Zhang, Q. Hu, E. A. Braunlin, L. J. Suggs, J. Zhang, *Tissue Eng. Part A* **2008**, *14*, 1025.
- [6] B. A. Aguado, W. Mulyasasmita, J. Su, K. J. Lampe, S. C. Heilshorn, *Tissue Eng. Part A* **2012**, *18*, 806.
- [7] M. J. Webber, J. Tongers, M. A. Renault, J. G. Roncalli, D. W. Losordo, S. I. Stupp, *Acta Biomater.* **2010**, *6*, 3.
- [8] T. Kofidis, D. R. Lebl, E. C. Martinez, G. Hoyt, M. Tanaka, R. C. Robbins, *Circulation* **2005**, *112*, 1173.
- [9] J. M. Singelyn, J. A. DeQuach, S. B. Seif-Naraghi, R. B. Littlefield, P. J. Schup-Magoffin, K. L. Christman, *Biomaterials* **2009**, *30*, 5409.
- [10] B. D. Olsen, J. A. Kornfield, D. A. Tirrell, *Macromolecules* **2010**, *43*, 9094.
- [11] H. D. Lu, M. B. Charati, I. L. Kim, J. A. Burdick, *Biomaterials* **2012**, *33*, 2145.
- [12] J. P. Schneider, D. J. Pochan, B. Ozbas, K. Rajagopal, L. Pakstis, J. Kretsinger, *J Am. Chem. Soc.* **2002**, *124*, 15030.
- [13] F. Cao, A. H. Sadrzadeh Rafie, O. J. Abilez, H. Wang, J. T. Blundo, B. Pruitt, C. Zarins, J. C. Wu, *J Tissue Eng. Regen. Med.* **2007**, *1*, 465.
- [14] N. Landa, L. Miller, M. S. Feinberg, R. Holbova, M. Shachar, I. Freeman, S. Cohen, J. Leor, *Circulation* **2008**, *117*, 1388.
- [15] M. A. Serban, Y. Liu, G. D. Prestwich, *Acta Biomater.* **2008**, *4*, 67.
- [16] J. H. Collier, J. S. Rudra, J. Z. Gasiorowski, J. P. Jung, *Chem. Soc. Rev.* **2010**, *39*, 3413.
- [17] C. T. Wong Po Foo, J. S. Lee, W. Mulyasasmita, A. Parisi-Amon, S. C. Heilshorn, *Proc. Natl. Acad. Sci. USA* **2009**, *106*, 22067.
- [18] W. Mulyasasmita, J. S. Lee, S. C. Heilshorn, *Biomacromolecules* **2011**, *12*, 3406.
- [19] W. P. Russ, D. M. Lowery, P. Mishra, M. B. Yaffe, R. Ranganathan, *Nature* **2005**, *437*, 579.
- [20] P. A. Zuk, M. Zhu, P. Ashjian, D. A. De Ugarte, J. I. Huang, H. Mizuno, Z. C. Alfonso, J. K. Fraser, P. Benhaim, M. H. Hedrick, *Mol. Biol. Cell* **2002**, *13*, 4279.
- [21] B. A. Bunnell, M. Flaas, C. Gagliardi, B. Patel, C. Ripoll, *Methods* **2008**, *45*, 115.
- [22] N. Sun, N. J. Panetta, D. M. Gupta, K. D. Wilson, A. Lee, F. Jia, S. Hu, A. M. Cherry, R. C. Robbins, M. T. Longaker, J. C. Wu, *Proc. Natl. Acad. Sci. USA* **2009**, *106*, 15720.
- [23] J. T. Connelly, A. J. Garcia, M. E. Levenston, *J. Cell. Physiol.* **2008**, *217*, 145.
- [24] P. E. de Almeida, J. R. van Rappard, J. C. Wu, *Am. J. Physiol. Heart Circ. Physiol.* **2011**, *301*, H663.
- [25] C. H. Contag, B. D. Ross, *J. Magn. Reson. Imaging* **2002**, *16*, 378.
- [26] J. D. Roh, R. Sawh-Martinez, M. P. Brennan, S. M. Jay, L. Devine, D. A. Rao, T. Yi, T. L. Mirensky, A. Nalbandian, B. Udelsman, N. Hibino, T. Shinoka, W. M. Saltzman, E. Snyder, T. R. Kyriakides, J. S. Pober, C. K. Breuer, *Proc. Natl. Acad. Sci. USA* **2010**, *107*, 4669.
- [27] F. Lu, H. Mizuno, C. A. Uysal, X. Cai, R. Ogawa, H. Hyakusoku, *Plast. Reconstr. Surg.* **2008**, *121*, 50.
- [28] D. Garcia-Olmo, D. Herreros, I. Pascual, J. A. Pascual, E. Del-Valle, J. Zorrilla, P. De-La-Quintana, M. Garcia-Arranz, M. Pascual, *Dis. Colon. Rectum* **2009**, *52*, 79.